Journal of Solid State Chemistry 188 (2012) 44–49

Contents lists available at SciVerse ScienceDirect

Journal of Solid State Chemistry

journal homepage: www.elsevier.com/locate/jssc

High-throughput and in situ EDXRD investigation on the formation of two new metal aminoethylphosphonates – $Ca(O_3PC_2H_4NH_2)$ and $Ca(OH)(O_3PC_2H_4NH_3)\cdot 2H_2O$

Corinna Schmidt [a], Mark Feyand [a], André Rothkirch [b], Norbert Stock [a,*]

[a] Institut für Anorganische Chemie, Christian-Albrechts-Universität, Max-Eyth Straße 2, D 24118 Kiel, Germany
[b] HASYLAB, DESY Hamburg, Notkestraße 85, 22607 Hamburg, Germany

ARTICLE INFO

Article history:
Received 2 November 2011
Received in revised form
15 January 2012
Accepted 22 January 2012
Available online 30 January 2012

Keywords:
Crystal growth
In situ EDXRD
Solvothermal
High-throughput
Crystal structure

ABSTRACT

The system Ca^{2+}/2-aminoethylphosphonic acid/H_2O/NaOH was systematically investigated using high-throughput methods. The experiments led to one new compound $Ca(O_3PC_2H_4NH_2)$ (**1**) and the crystal structure was determined using in house X-ray powder diffraction data (monoclinic, $P2_1/c$, $a=9.7753(3)$, $b=6.4931(2)$, $c=8.4473(2)$ Å, $\beta=106.46(2)^\circ$, $V=514.20(2)$ Å^3, $Z=4$). The formation of **1** was investigated by in situ energy dispersive X-ray diffraction measurements (EDXRD) at beamline F3 at HASYLAB (light source DORIS III), DESY, Hamburg. An intermediate, $Ca(OH)(O_3PC_2H_4NH_3)\cdot 2H_2O$ (**2**), was observed and could be isolated from the reaction mixture at ambient temperatures by quenching the reaction. The crystal structure of **2** was determined from XRPD data using synchrotron radiation (monoclinic, $P2_1/m$, $a=11.2193(7)$, $b=7.1488(3)$, $c=5.0635(2)$ Å, $\beta=100.13(4)^\circ$, $V=399.78(3)$ Å^3, $Z=2$).

1. Introduction

Inorganic–organic hybrid compounds have gained increased attention during the last years, due to their structural diversity and their potential application, for example in catalysis, gas storage or gas separation [1,2]. Most of these compounds contain polycarboxylate, -phosphonate or -sulfonate ions as linker molecules [3–5]. The use of polyfunctionalized linker molecules with different functionalities has also been investigated and various metal phosphonocarboxylates [6–9] and -phosphonosulfonates [10–12] have been described. Aminomethylsphosphonic acid of secondary and tertiary amines have been successfully applied for various dense metal phosphonates [4,13] as well as porous compounds such as MIL-91 [14], STA-12 [15], and STA-16 [16]. The use of aminoalkylphosphonic acids of primary amines (H_2N–C_nH_{2n}–PO_3H_2) for the synthesis of inorganic–organic hybrid compounds is far less developed.[17–24] While various metal aminomethylposphonates (M=Zn^{2+}, Cd^{2+}, Pb^{2+}, Hg^{2+}, Ag^{+}) [17] and metal aminoethylphosphonates (M=Zn^{2+} [18], Cd^{2+} [19], Cu^{2+} [20], Co^{2+} [21], Cr^{2+} [22]) have been reported, the number of metal aminopropylphosphonates (M=Zr^{4+} [23], Al^{3+} [24]) is rather limited. Although a variety of metal ions have been incorporated, these aminoalkylphosphonates crystallize exclusively in layered or pillared layered structures. In all cases, the phosphonate group is connected to the metal ions and the amino group either coordinates to the metal ions, or it is protonated and protrudes into the interlayer space. In metal aminoethylphosphonates three structural motives are observed: (1) the coordination of the amino group to the metal ions result in pillared layered structures [18,19,21], (2) the protonation of the amino group results in layered structures, where chloride or sulfate ions are located between the layers [20,22], or (3) the amino group coordinates to the metal center within a metal phosphonate layer and simultaneously nitrate ions are located between the layers [20].

The discovery of new inorganic–organic hybrid compounds can be accelerated using high-throughput (HT) methods. The HT methodology enables an efficient and fast investigation of multi-parameter synthesis fields, thus the influence of the pH, the molar ratios of the starting materials, the reaction temperature and the solvents on the product formation can easily be determined [25–27]. Therefore, it allows us to rapidly discover new compounds, to optimize the synthesis conditions and to establish reaction trends.

Although the HT methodology enables an extensive investigation of large synthesis fields, no information on the formation of the compounds is obtained. Time resolved in situ EDXRD measurements are the method of choice to learn more about the crystallization process. This method has been employed to study the formation of zeolites [28], thioantimonates [29], and metal phosphonoalkylsulfonates [30], under solvothermal conditions. Recently, the studies were extended to inorganic–organic hybrid compounds, such as the metal organic frameworks, HKUST-1 ($[Cu_3(BTC)_2]\cdot 3H_2O$ (BTC=1,3,5-benzenetricarboxylate)) [31], Fe-MIL-53 ($[Fe(OH)(O_2C$–C_6H_4–$CO_2]\cdot H_2O$)

* Corresponding author. Fax: +49 431 880 1775.
E-mail address: stock@ac.uni-kiel.de (N. Stock).

0022-4596/$ - see front matter © 2012 Elsevier Inc. All rights reserved.
doi:10.1016/j.jssc.2012.01.044

[31], MOF-14 ($Cu_3(BTB)_2(H_2O)_3 \cdot (DMF)_9(H_2O)_2$, (BTB=4,4′,4″-benzene-1,3,5-triyl–tribenzoic acid)) [32], Al-MIL-101-NH_2 ($Al_3O(DMF)[(OOC)C_6H_3NH_2(COO)]_3 \cdot xH_2O$ [33], CAU-1-$(OH)_2$ ($[Al_8(OH)_4(OCH_3)_8(BDC(OH)_2)_6] \cdot xH_2O$ (BDC=1,4-benzenedicarboxylate)) [34] and CAU1-NH_2 ($([Al_8(OH)_4(OCH_3)_8(BDC(NH_2))_6] \cdot xH_2O$) [35]. In situ EDRXD measurements enable to monitor the crystallization process and therefore possible intermediates can also be observed. In some cases the intermediate can be isolated by quenching of the reaction mixture [31,33].

Although a number of metal ions have been investigated, there are no results on the use of alkaline earth metals for the formation of metal aminophosphonate hybrid compounds. Therefore, we have started a systematic investigation of these systems by carrying out a metal screening experiment. Based on these results, we have chosen Ca^{2+} as the metal ion of choice for more in depth studies. Here we present our results of the systematic HT investigation of the system Ca^{2+}/AEPA/H_2O/NaOH (AEPA=2-aminoethylphosphonic acid) and the time resolved in situ EDXRD study of the synthesis of $Ca(O_3PC_2H_4NH_2)$.

2. Material and methods

The synthesis of 2-aminoethylphosphonic acid was performed based on reported procedures [36–38]. All reagents and solvents were purchased from commercial sources. They were of analytical grade and were used as obtained. HT X-ray powder diffraction (XRPD) measurements were performed on a Stoe Stadi P HT – diffractometer in transmission geometry with Cu $K_{\alpha 1}$ radiation and equipped with an image plate detector system. MIR spectra were collected on a Bruker Alpha spectrometer equipped with a diamond ATR unit in the spectral range of 4000–400 cm^{-1}. Raman spectra were recorded using a Bruker FRA 106 Raman spectrometer. The thermogravimetric analysis was executed with a NETSCH STA 409 CD analyzer, under air (75 mL/min), with a heating rate of 2 K/min. Elemental analyses were carried out using a Eurovektor EuroEA Elemental Analyzer. The in situ EDXRD measurements were performed at beamline F3 at HASYLAB, DESY, Hamburg.

2.1. High-throughput experiments

Applying our HT method the system Ca^{2+}/AEPA/H_2O/NaOH was investigated under solvothermal reaction conditions. All starting materials were applied as aqueous solutions. The reaction block was heated to 130 °C in 2 h. After 48 h at the reaction temperature, the multiclave was cooled down within 12 h. A custom made HT reactor was employed containing 48 PTFE vessels each with a maximum volume of 300 μL. The molar ratios Ca^{2+}:AEPA were varied from 0.17 to 6.5:1. The amount of NaOH was varied from 0.17 to 6:1 (NaOH:AEPA). The starting materials were added to the PFTE vessels in the following order: AEPA, $Ca(NO_3)_2 \cdot 4H_2O$, H_2O and NaOH. The reaction products were filtered off, washed with water and dried in air. All samples were characterized by XRPD measurements. The concentrations of the starting solutions and the exact amounts of the starting materials employed are given in Table S1 in the Supporting Information.

2.2. Synthesis of $Ca(O_3PC_2H_4NH_2)$ (1)

A single phase microcrystalline powder of **1** was obtained from the HT investigation by mixing 40 μL (40 μmol) of a 1 M aqueous solution of AEPA, 40 μL of a 2 M aqueous solution of $Ca(NO_3)_2 \cdot 4H_2O$, 90 μL H_2O and 30 μL of a 4 M aqueous solution of NaOH (molar ratio Ca^{2+}:AEPA:NaOH=2:1:3). Scale-up synthesis using Schott Duran glass culture tubes (5 mL) were performed to get larger amounts of **1**. Therefore, the tenfold amount of the starting materials and the same temperature program were used. The purity was confirmed by the elemental analyses ((%) calcd. for $CaPNC_2 \cdot H_6O_3$: C: 14.73, N: 8.59, H: 3.71; found: C: 15.31, N: 8.23, H: 3.42) and the successful structure refinement of the XRPD data.

2.3. Synthesis of $Ca(OH)(O_3PC_2H_4NH_3) \cdot 2H_2O$ (2)

Compound **2** was observed as an intermediate during the in situ EDXRD investigation. Based on these results the compound was obtained executing the scale up synthesis of **1** at room temperature under stirring and quenching the reaction mixture after 1 h by filtration. The synthesis resulted in a microcrystalline colorless powder. The purity was confirmed by the elemental analyses ((%) calcd. for $CaPNC_2H_{12}O_6$: C: 11.06, N: 6.45, H: 5.57; found: C: 10.85, N: 6.28, H: 3.95) and the successful structure refinement of the XRPD data.

2.4. In situ EDXRD investigation

The EDXRD investigation was performed at HASYLAB, beamline F3 using the light source DORIS III at DESY in Hamburg, Germany. White synchrotron radiation was used in combination with a germanium detector system cooled with liquid nitrogen. The detector angle was set to approximately 1.9° and the collimator to 0.2×0.2 mm^2. The reaction was carried out in Schott Duran glass culture tube (5 mL) placed in a custom-made reactor system heated by an external thermostat to 130 °C [39]. To investigate the formation of **1** the optimized reaction conditions obtained from the HT investigation and the scale-up synthesis were used. The starting materials were employed as aqueous solutions (300 μL 1 M AEPA, 300 μL 2 M $Ca(NO_3)_2 \cdot 4H_2O$, 2.175 mL water and 225 μL 4 M NaOH (Ca^{2+}:AEPA:NaOH=2:1:3) which was stirred during the reaction. The exposure time for each EDXRD spectrum was 60 s.

2.5. Structure determination

The structure determination of $Ca(O_3PC_2H_4NH_2)$ (**1**) was accomplished using in house XRPD data. The XRPD measurement was performed on a STOE Stadi-P powder diffractometer in transmission geometry with Cu $K_{\alpha 1}$ radiation (λ=154.0598 pm) equipped with a position-sensitive detector. Indexing of the XRPD pattern of **1** was accomplished using the program EXPO2009 [40] and cell parameters were refined applying the program WinXPOW [41] (FOM: 36.4). The structure determination of $Ca(OH)(O_3PC_2H_4NH_3) \cdot 2H_2O$ (**2**) was accomplished using synchrotron data. The synchrotron measurement was performed at HASYLAB, beamline G3 at DESY in Hamburg, Germany using monochromatic light (λ=154.302 pm) [42]. The powder pattern was indexed applying the program TOPAS [43] and cell parameters were refined using WinXPOW [41] (FOM: 37.5). Structure determinations were carried out with the program EXPO 2009 using direct methods. All atoms were observed in the structure solution and the atomic coordinates were set as the starting model for the Rietveld refinement applying the program TOPAS. The Rietveld refinement involved the following parameters for compound **1**: 4 cell parameters, 24 atomic coordinates (Table S2), 1 overall thermal factor, 1 scale factor, 1 zero point and 15 background parameters. For compound **2**: 4 cell parameters, 30 atomic coordinates (Table S3), 1 overall thermal factor, 1 scale factor, 1 zero point and 7 background parameters were used for the Rietveld refinement. Preferred orientation was modeled using spherical harmonics series. Restrains were applied to the P–O, P–C, C–C and C–N bond lengths and to the O–P–C and C–C–N

Table 1
Summary of crystal data and refined structure parameters for $Ca(O_3PC_2H_4NH_2)$ (**1**) and $Ca(OH)(O_3PC_2H_4NH_3)\cdot 2H_2O$ (**2**).

	Compound 1	**Compound 2**
Formula	$C_2H_6O_3PNCa$	$C_2H_{12}O_6PNCa$
Weight (g/mol)	163.12	217.17
Crystal system	Monoclinic	Monoclinic
Space group	$P2_1/c$ (No. 14)	$P2_1/m$ (No. 11)
a (pm)	9.7753(3)	11.2193(7)
b (pm)	6.4931(2)	7.1488(3)
c (pm)	8.4473(2)	5.0635(2)
β (°)	106.46(2)	100.13(4)
V (Å^3)	514.20(2)	399.78(3)
Z	4	2
R_{wp}	0.0697	0.0502
R_{exp}	0.0397	0.0171
R_{Bragg}	0.0331	0.0221
GOF	1.754	2.944

bond angles in both compounds. For compound **2** restrains were applied in addition to the O–O and O–N distances. The results of the final Rietveld refinements are shown in Figs. 2 and 5 for **1** and **2**, respectively. Results of the crystallographic work are summarized in Table 1. Selected bond lengths and angles are summarized in Tables S4 and S5. Crystallographic data (excluding structure factors) for the structures in this paper have been deposited with the Cambridge Crystallographic Data Centre as supplementary publication nos. CCDC-847095 and 847096 for **1** and **2**, respectively. Copies of the data can be obtained, free of charge, on application to CCDC, 12 Union Road, Cambridge CB2 1EZ, UK (fax: +44 1223 336033 or email: deposit@ccdc.cam.ac.uk).

3. Results and discussion

The system Ca^{2+}/AEPA/H_2O/NaOH was systematically investigated applying our high-throughput methodology. Therefore the molar ratio of the starting materials was varied stepwise. Based on the XRPD measurements of the resulting products a ternary crystallization diagram can be set up, which is shown in Fig. 1.

The HT experiment using 2-aminoethylphosphonic acid resulted in one new compound. Crystalline products of $Ca(O_3PC_2H_4NH_2)$ were obtained at molar ratios Ca^{2+}:AEPA:NaOH = 0.5–6.5:1:1.5–4, i.e., in the pH range $\sim 8 < pH < 13$. In a large field of formation, i.e., in the pH range $\sim 6 < pH < 7$ no precipitate was obtained. These results are marked in white in the ternary diagram. At pH = 14 the experiment led to X-ray amorphous products (black points). The product obtained at a molar ratio Ca^{2+}:AEPA:NaOH = 2:1:3 was used for the structure determination.

3.1. Crystal structure of $Ca(O_3PC_2H_4NH_2)$ (1)

The crystal structure of **1** was determined from in house XRPD data. The final Rietveld plot is shown in Fig. 2.

Compound **1** contains one Ca^{2+} ion and one $(O_3PC_2H_4NH_2)^{2-}$ ion in the asymmetric unit. The coordination sphere of the calcium ion contains five linker molecules. The Ca^{2+} ion is surrounded by six oxygen atoms of the phosphonate groups and one nitrogen atom of the amino group which results in CaO_6N-polyhedra (Fig. 3, left). Each linker molecule is coordinated to five Ca^{2+} ions. While O3 and N1 act as monodentate ligands, O1 and O2 act as μ_2 and μ_3 bridging ligand atoms, respectively (Fig. 3, right).

Each CaO_6N–polyhedron is connected to three other CaO_6N–polyhedra via common edges. This leads to six-rings and layers are formed in the *b*,*c*-plane (Fig. 4, left). The $-C_2H_4-$ unit of the linker molecule is involved in the interconnection of the CaO_6N-

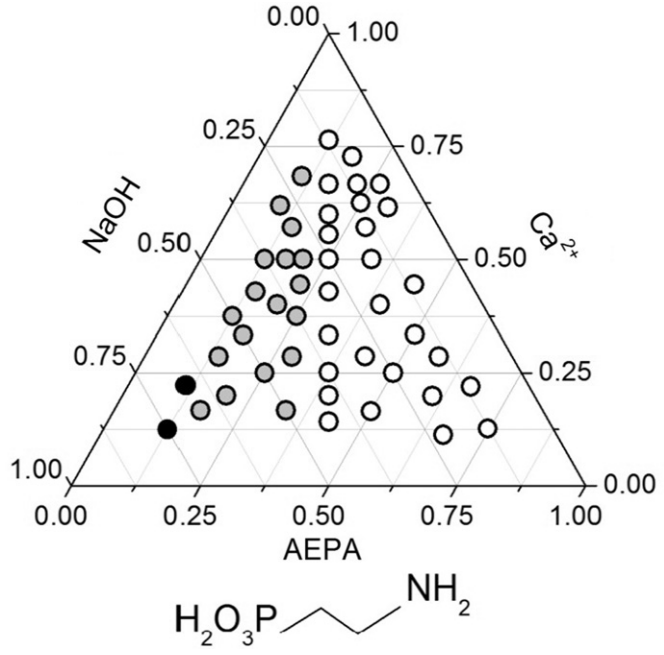

Fig. 1. Crystallization diagram of the system Ca^{2+}/AEPA/H_2O/NaOH.. Title compound **1** ($Ca(O_3PC_2H_4NH_2)$) is marked in gray, X-ray amorphous products and no precipitate are marked in black and white, respectively.

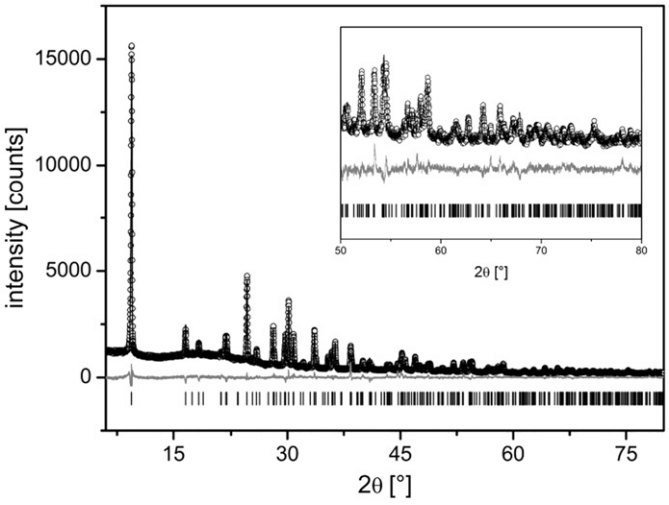

Fig. 2. Observed (○) and Rietveld refined XRPD pattern (black line) of compound **1**. The residual (difference plot of the measured vs. refined pattern) is presented by the gray line. The vertical lines below the patterns indicate the Bragg positions.

polyhedra wihtin each layer. These layers are connected to each other through van der Waals interactions (Fig. 4, right).

3.2. Crystal structure of $Ca(OH)(O_3PC_2H_4NH_3)\cdot 2H_2O$ (2)

The crystal structure of compound **2** was determined from synchrotron data. The final Rietveld plot is shown in Fig. 5.

The localization of the H-atoms is based on previously reported crystal structures of metal aminoethyl- and aminopropylphosphonates [18–24] in combination with the results of the IR spectroscopic and the thermogravimetric measurements. Thus, the crystal structure of **2** contains one Ca^{2+} ion, one linker molecule and one hydroxide ion as well as two water molecules per formula unit. The Ca^{2+} ion is surrounded by six oxygen atoms and CaO_6-polyhedra are formed (Fig. 6, left). Each linker molecule is coordinated to four Ca^{2+} ions. While both oxygen atoms O1 are connected to one Ca^{2+} ion, the

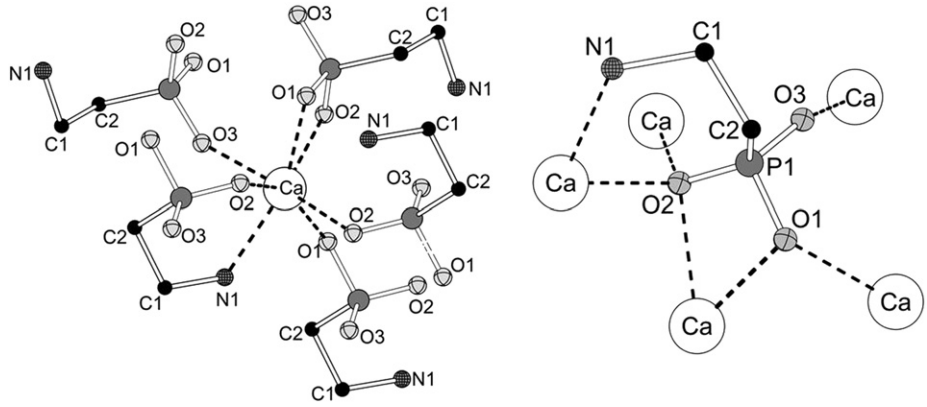

Fig. 3. Coordination sphere of the Ca^{2+} ion in $Ca(O_3PC_2H_4NH_2)$ (**1**) (left). Coordination scheme of the linker molecule to the Ca^{2+} ions (right).

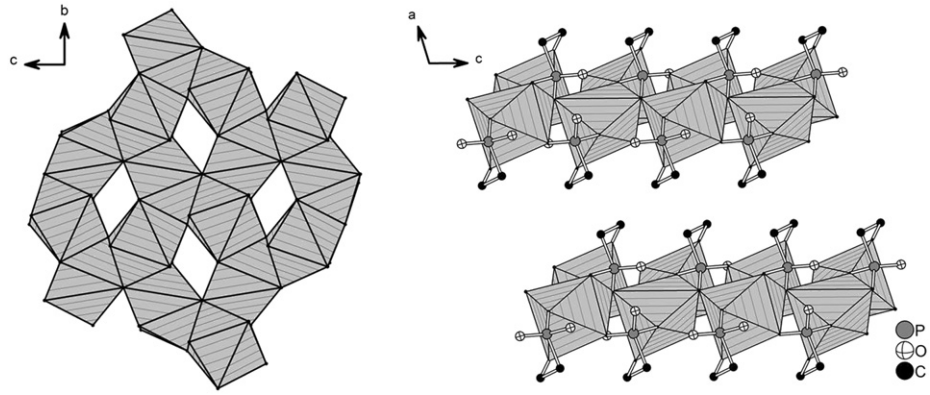

Fig. 4. Left: layer composed of edge-sharing CaO_6N-polyhedra in the *b*,*c*-plane. Right: layers in $Ca(O_3PC_2H_4NH_2)$ are interconnected by van der Waals interactions.

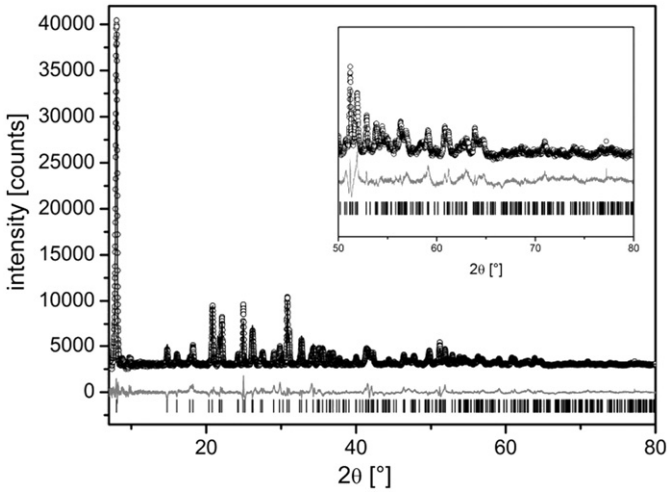

Fig. 5. Observed (○) and Rietveld refined XRPD pattern (black line) of compound **2**. The residual (difference plot of the measured vs. refined pattern) is presented by the gray line. The vertical lines below the patterns indicate the Bragg positions.

oxygen atom O2 acts as bridging atom. Edge-sharing of the CaO_6-polyhedra through O2 and the hydroxide ions results in chains along the *b*-axis (Fig. 6, right). In the vicinity of the oxygen atoms O1 water molecules (OW1) are observed, which act as H-donors in hydrogen bonds to O1 (D–A=236.7(5)). The hydroxide ion OH is involved in hydrogen bonds to OW1 as the H-donor with a bond distance of D–A=279.2(21) pm.

The Ca–O chains are connected via the phosphonate groups to build layers in the *b*,*c*-plane (Fig. 7, left). Although a hydroxide ion is part of the structure, the amino group should be protonated due to the charge equalization. The presence of $-NH_3^+$ groups is supported by the fact that the $-C_2H_4NH_3^+$ units of the linker molecules point into the interlayer region where water molecules are located (OW2). The nitrogen atoms interact in hydrogen bonds as H-aceptor and N1–OW2 bond distances of 286.1(19) and 279.6(17) pm are observed (Fig. 7, right). In addition hydrogen bonds between OW2 and OW1 are found with a length of 261.6(9) pm. The anticipated hydrogen bonding scheme as well as the bond lengths and angles are given in the Supporting Informations (Fig. S1, Tables S5 and S6).

Both compounds **1** and **2** are composed of layers. While edge-sharing of CaO_6N-polyhedra leads to six-rings in the layers of $Ca(O_3PC_2H_4NH_2)$ (**1**), the layers in $Ca(OH)(O_3PC_2H_4NH_3)\cdot 2H_2O$ (**2**) contain of edge-sharing CaO_6-polyhedra. In compound **2** hydroxide ions are involved in the connection of the Ca^{2+} ions. While the nitrogen atom in **1** is part of the coordination sphere of the Ca^{2+} ion, the amino groups in compound **2** are protonated and point into the interlayer space. The crystal structure of **2** is completed by two water molecules per formula unit. One water molecule (OW1) is located close to the Ca–O-layers and interacts in hydrogen bonds to the hydroxide ion, the phosphonate group and OW2. The second water molecule (OW2) is located in the interlayer space and there involved into hydrogen bonds with the nitrogen atoms.

3.3. Spectroscopic and thermal investigations

Compounds **1** and **2** were studied by infrared and Raman spectroscopy (Figs. S2 and S3). All compounds show the typical bands of the P–C and P–O stretching vibrations of the CPO_3-group in the region 1130–950 cm^{-1}. For compound **1**, the characteristic bands at

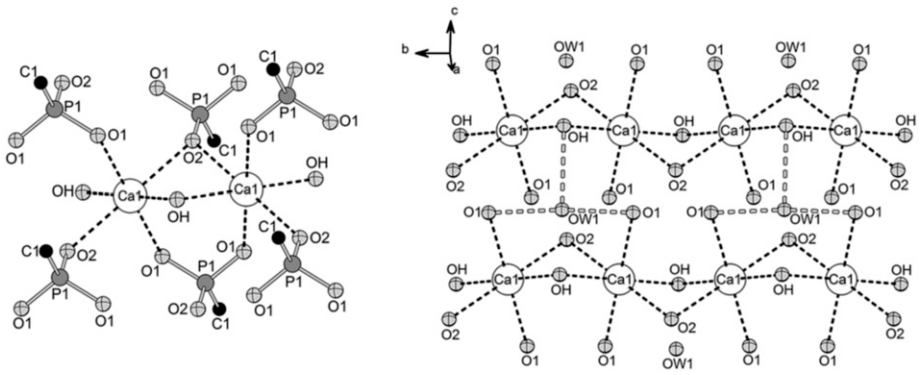

Fig. 6. Left: coordination sphere of the Ca^{2+} ions in $Ca(OH)(O_3PC_2H_4NH_3)\cdot 2H_2O$ (**2**). Right: chain of edge-sharing CaO_6-polyhedra along the *b*-axis. Hydrogen bonds between OW1, O1 and OH are observed (white dotted lines).

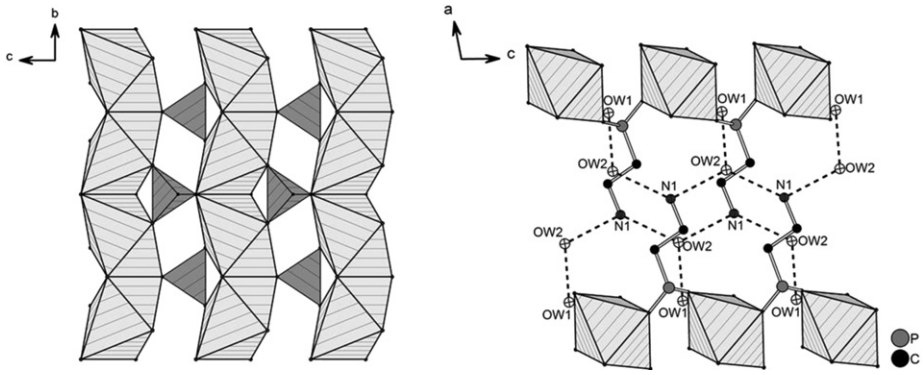

Fig. 7. Left: layer of chains of edge-sharing CaO_6-polyhedra (shaded in light gray) and PO_3C-polyhedra (shaded in dark gray). OW1 and hydrogen bonds are omitted for clarity. Right: the $-C_2H_4NH_3$ units of the linker molecules point into the interlayer space. Hydrogen bonds (dotted lines) are observed between the water molecules OW1 and OW2 as well as OW2 and N1. Hyrogen bonds between OW1, O1 and OH are omitted for clarity.

3358–3288 cm^{-1} and 1591 cm^{-1} for the stretching and deformation vibration of the amino group are observed, respectively. The vibration bands at 2900–2845 cm^{-1} and 1476 cm^{-1} correspond to the C–H stretching and deformation vibration of the CH_2-group. The C–N-stretching vibration results in a band at 1217 cm^{-1}. Compound **2** shows the characteristic vibration band at 3645–3600 cm^{-1} of bridging hydroxide ions. The bands for the stretching and deformation vibration of the protonated amino group are observed at 3331–3162 cm^{-1} and 1594 cm^{-1}. In comparison to the corresponding vibrations of compound **1** they are slightly weaker due to the protonation and the presence of hydrogen bonds. The bands at 2950–2890 cm^{-1} and 1475 cm^{-1} are related to the vibrations bands of the CH_2-groups. The water molecules in the crystal structure lead to the broadening of the bands at 3250 cm^{-1} and 1590 cm^{-1}.

Thermogravimetric (TG) measurements up to 860 °C for **1** and 900 °C for **2** under air flow using a heating rate of 2 K/min were performed to gain deeper insight into the thermal stability of the compounds. The thermal degradation of compound **1** takes place in 3 steps in the range of 195–850 °C. A total weight loss of 25.6% is observed (calc.: 27.0%) which leads, based on XRPD measurements, to $Ca_2P_2O_7$. For compound **2** a multistep thermal degradation is observed. Up to 215 °C a weight loss of 14.5% is observed which corresponds to the loss of two water molecules per formula unit (calc.: 16.5%). A total weight loss of 38.7% is measured up to 900 °C, which results in a X-ray amorphous product. The TG curves are presented in the Supporting Information (Figs. S4 and S5).

3.4. In situ EDRXD investigation

Although the HT experiment allows an efficient investigation of multiparameter fields and therefore the rapid discovery of new compounds, no information about the crystallization itself or possible crystalline intermediates are obtained. Thus the formation of compound **1** was investigated by in situ EDXRD measurements at 130 °C using conventional heating [39]. The reactants were employed as previously described. For an evaluation of the data, the reaction progress $\alpha(t)=I(t)/I(t_\infty)$ was determined, where I is the intensity at a given time t and at the end of the reaction t_∞, respectively. The intensity I was obtained by integrating the 100 reflection of **1** and **2** (maximum error 6%). The surface plot and the reaction progress $\alpha(t)$ are shown in Fig. 8.

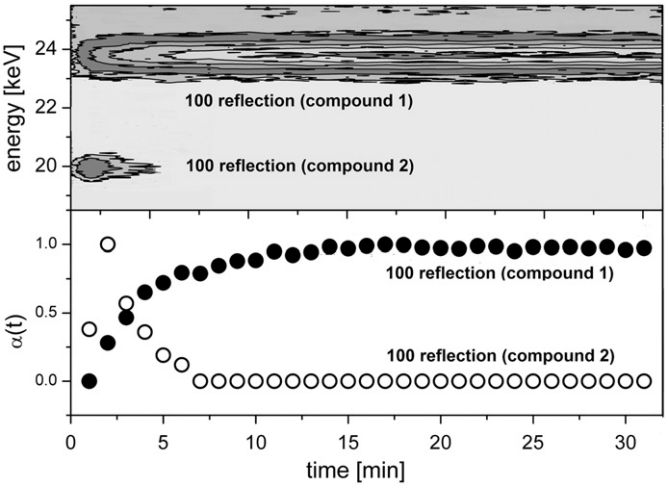

Fig. 8. Surface plot and normalized intensities of the 100 reflections of the formation of $Ca(O_3PC_2H_4NH_2)$ (**1**) and $Ca(OH)(O_3PC_2H_4NH_3)\cdot 2H_2O$ (**2**).

The surface plot shows two signals at 20 keV and 24 keV. This energy range corresponds under the given experimental settings to the 2θ range of 7 to 10.5°. The signal at 24 keV corresponds to the 100 reflection of compound **1** and is observed for the first time after 1 min. It reaches a maximum after 14 min. The second signal at 20 keV is immediately detected and reaches a maximum after 2 min. After 2 min the signal at 20 keV (marked in white) decreases and simultaneously the signal of the 100 reflection of $Ca(O_3PC_2H_4NH_2)$ (**1**) increases (marked in black). This reaction progress shows that the formation of compound **1** involves a formation of an intermediate. The curves of the reaction progress of **1** and **2** intersects at $\alpha(t)=0.5$. This suggests a direct transformation of the intermediat to the final product via a solid-solid transformation [44]. The intermediate was indentified as $Ca(OH)(O_3PC_2H_4NH_3)\cdot 2H_2O$ (**2**) and the signal at 20 keV corresponds to the 100 reflection. The comparison of the EDXRD spectrum and the XRPD patterns of $Ca(O_3PC_2H_4NH_2)$ (**1**) and the intermediate $Ca(OH)(O_3PC_2H_4NH_3)\cdot 2H_2O$ (**2**) is shown in the Supporting Informations (Fig. S6). The determined densities of the title compounds give a further indication for the formation of the intermediate as the kinetically stable product. While a density of 1.703(1) g cm^{-3} was determined for compound **2** as the kinetically stable intermediate, the determination of the density led to 2.029(1) g cm^{-3} for compound **1** as the thermodynamically stable product.

4. Conclusion

Using a combination of different synthesis and characterization tools such as high-throughput method as well as in situ EDXRD and high resolution XRPD measurements the reaction system Ca^{2+}/AEPA/H_2O/NaOH was studied in detail. While the HT methods demonstrated the existence of the new compound $Ca(O_3PC_2H_4NH_2)$ in a large fraction of the crystallization diagram, the in situ EDXRD experiment showed that the crystallizaion is completed after 14 min at 130 °C. In addition, the existence of a crystalline intermediate was observed. The high-resolution XRPD data using synchrotron radiation allowed us to determine its crystal structure.

Supporting information

Supporting Information with exact amounts used for the high-throughput syntheses, Atomic parameter for the Rietveld refinement, selected bond lengths and angles, IR spectrum and TG measurement, selected bond lengths and angles and the in situ study are available. This information is available free of charge via the Internet at http://pubs.acs.org/.

Acknowledgment

We thank the HASYLAB / DESY, Hamburg for the allocated beam time at the light source DORIS III (proposal number I-20100288), Ursula Cornelissen and Stephanie Pehlke for spectroscopic measurements, Beatrix Seidlhofer and Nicola Herzberg for TG/DTA measurements and the group of Prof. Dr. Wolfgang Bensch for the allocation of the reactor system for the in situ EDXRD studies.

Appendix A. Supporting materials

Supplementary data associated with this article can be found in the online version at doi:10.1016/j.jssc.2012.01.044.

References

[1] K.K. Tanabe, S.M. Cohen, Inorg. Chem. 49 (2010) 6766.
[2] A.U. Czaja, N. Trukhan, U. Müller, Chem. Soc. Rev. 38 (2009) 1284.
[3] J.L. Rowsell, O.M. Yaghi, Microporous Mesoporous Mater. 73 (2004) 3.
[4] G.K.H. Shimizu, R. Vaidhyanathan, J.M. Taylor, Chem. Soc. Rev. 38 (2009) 1430.
[5] A. Clearfield, Prog. Inorg. Chem. 47 (1998) 371.
[6] S. Bauer, T. Bein, N. Stock, J. Solid State Chem. 179 (2006) 145.
[7] S. Bauer, T. Bein, N. Stock, Inorg. Chem. 44 (2005) 5882.
[8] N. Stock, S.A. Frey, G.D. Stucky, A.K. Cheetham, J. Chem. Soc., Dalton Trans. (2000) 4292.
[9] T.-B. Liao, Y. Ling, Z.-X. Chen, Y.-M. Zhou, L.-H. Weng, Chem. Commun. 46 (2010) 1100.
[10] A. Sonnauer, M. Feyand, N. Stock, Cryst. Growth Des. 9 (2008) 586.
[11] A. Sonnauer, N. Stock, J. Solid State. Chem. 181 (2008) 473.
[12] Z.-Y. Du, H.-B. Xu, X.-L. Li, J.-G. Mao, Eur. J. Inorg. Chem. (2007) 4520.
[13] N. Stock, A. Stoll, T. Bein, Microporous Mesoporous Mater. 69 (2004) 65.
[14] C. Serre, J.A. Groves, P. Lightfoot, A.M.Z. Slawin, P.A. Wright, N. Stock, T. Bein, M. Haouas, F. Taulelle, G. Ferey, Chem. Mater. 18 (2006) 1451.
[15] S.R. Miller, G.M. Pearce, P.A. Wright, F. Bonino, S. Chavan, S. Bordiga, I. Margiolaki, N. Guillou, G. Ferey, S. Bourrelly, P.L. Llewellyn, J. Am. Chem. Soc. 130 (2008) 15967.
[16] M.T. Wharmby, J.P.S. Mowat, S.P. Thompson, P.A. Wright, J. Am. Chem. Soc. 133 (2011) 1266.
[17] C.R. Samanamu, E.N. Zamora, J.-L. Montchamp, A.F. Richards, J. Solid State Chem. 181 (2008) 1462.
[18] S. Drumel, P. Janvier, D. Deniaud, B. Bujoli, J. Chem. Soc., Chem. Commun. (1995) 1051.
[19] F. Fredoueil, D. Massiot, P. Janvier, F. Gingl, M. Bujoli-Doeuff, M. Evain, A. Clearfield, B. Bujoli, Inorg. Chem. 38 (1999) 1831.
[20] S. Drumel, P. Janvier, M. Bujoli-Doeuff, B. Bujoli, Inorg. Chem. 35 (1996) 5786.
[21] W.R. Gemmill, M.D. Smith, B.A. Reisner, J. Solid State Chem. 178 (2005) 2658.
[22] E.M. Bauer, C. Bellitto, M. Colaoietro, G. Portalone, G. Righini, Inorg. Chem. 42 (2003) 6345.
[23] G.L. Rosenthal, J. Caruso, Inorg. Chem. 31 (1992) 3104.
[24] N. Zakowsky, P.S. Wheatley, I. Bull, M.P. Attfield, R.E. Morris, Dalton Trans. (2001) 2899.
[25] N. Stock, T. Bein, Angew. Chem. Int. Ed. 116 (2004) 767.
[26] S. Bauer, N. Stock, Angew. Chem. Int. Ed. 46 (2007) 6857.
[27] N. Stock, T. Bein, J. Mater. Chem. 15 (2005) 1384.
[28] R.I. Walton, F. Millange, D. O'Hare, A.T. Davies, G. Sankar, C.R.A. Catlow, J. Phys. Chem. B 105 (2001) 83.
[29] R. Kiebach, N. Pienack, M.-E. Ordolff, F. Studt, W. Bensch, Chem. Mater. 18 (2006) 1196.
[30] M. Feyand, C. Näther, A. Rothkirch, N. Stock, Inorg. Chem. 49 (2010) 11158.
[31] F. Millange, M.I. Medina, N. Guillou, G. Férey, K.M. Golden, R.I. Walton, Angew. Chem. Int. Ed. 49 (2010) 763.
[32] F. Millange, R. El Osta, M.E. Medina, R.I. Walton, Cryst. Eng. Commun. 13 (2011) 103.
[33] J. Juan-Alcañiz, M. Goesten, A. Martinez-Joaristi, E. Stavitski, A.V. Petukhov, J. Gascon, F. Kapteijn, Chem. Commun. 47 (2011) 8578.
[34] T. Ahnfeldt, J. Moellmer, V. Guillerm, R. Staudt, C. Serre, N. Stock, Chem. Eur. J. 17 (2011) 6462.
[35] T. Ahnfeldt, N. Stock, CrystEngComm (2011). doi:10.1039/C1CE05956D.
[36] H. Becker, et al., Organikum, 22 Edition, Wiley-VCH, Weinheim, 2004, p. 600.
[37] J. Barycki, P. Mastalerz, M. Soroka, Tetrahedron Lett. 36 (1970) 3147.
[38] C. Wasielewski, M. Topolski, L. Dembkowski, J. Prakt. Chem. (1989) 507.
[39] L. Engelke, M. Schäfer, M. Schur, W. Bensch, Chem. Mater. 13 (2001) 1383.
[40] A. Altomare, M. Camalli, C. Cuocci, C. Giacovazzo, A. Moliterni, R. Rizzi, EXPO2009: structure solution by powder data in direct and reciprocal space, J. Appl. Cryst. 42 (2009) 1197.
[41] WinXPOW version 2.11, (2005), Stoe & Cie GmbH, Darmstadt, Germany.
[42] T. Wroblewski, O. Clauß, H.-A. Crostack, A. Ertel, F. Fandrich, Ch. Genzel, K. Hradil, W. Ternes, E. Woldt, Nucl. Instrum. Methods. A. 428 (1999) 570.
[43] A. Coelho, Topas V4.1, Academic version: General Profile and Structure Analysis Software for Powder Diffraction Data, Bruker AXS Ltd, (2004).
[44] R. Kiebach, N. Pienack, W. Bensch, J.-D. Grunwaldt, A. Michailovski, A. Baikar, T. Fox, Y. Zhou, G.R. Patzke, Chem. Mater. 20 (2008) 3022.